

CoCoG-2: Controllable generation of visual stimuli for understanding human concept representation

Chen Wei^{†,1,2}, Jiachen Zou^{†,1}, Dietmar Heinke², and Quanying Liu^{*,1}

¹Southern University of Science and Technology, Shenzhen, China

²University of Birmingham, Birmingham, United Kingdom

Abstract. Humans interpret complex visual stimuli using abstract concepts that facilitate decision-making tasks such as food selection and risk avoidance. Similarity judgment tasks are effective for exploring these concepts. However, methods for controllable image generation in concept space are underdeveloped. In this study, we present a novel framework called CoCoG-2, which integrates generated visual stimuli into similarity judgment tasks. CoCoG-2 utilizes a training-free guidance algorithm to enhance generation flexibility. CoCoG-2 framework is versatile for creating experimental stimuli based on human concepts, supporting various strategies for guiding visual stimuli generation, and demonstrating how these stimuli can validate various experimental hypotheses. CoCoG-2 will advance our understanding of the causal relationship between concept representations and behaviors by generating visual stimuli. The code is available at <https://github.com/ncc1ab-sustech/CoCoG-2>.

Keywords: Concept representation · Conditional generative model · Experimental design.

1 Introduction

Humans receive abundant visual stimuli in their daily lives. By understanding visual input’s abstract concepts such as function, edibility, and biological properties, humans can perform high-level cognitive decision-making tasks such as food selection and risk avoidance. A large number of human studies have shown that the similarity judgment task is an effective experimental paradigm for revealing human concept representation [15,13,21,7]. In the similarity judgment task, participants are required to evaluate various visual stimuli and make judgments based on the similarity of these images. Such similarity is measured in the concept space, rather than the original image space. So their distance in the concept space reflects the psychological space in the human mind [13,21]. The distance in main dimensions of concept representation can predict and explain human decision-making behaviors; in turn, similarity judgments are expected to reflect

[†] Equal contribution.

^{*} Corresponding author.

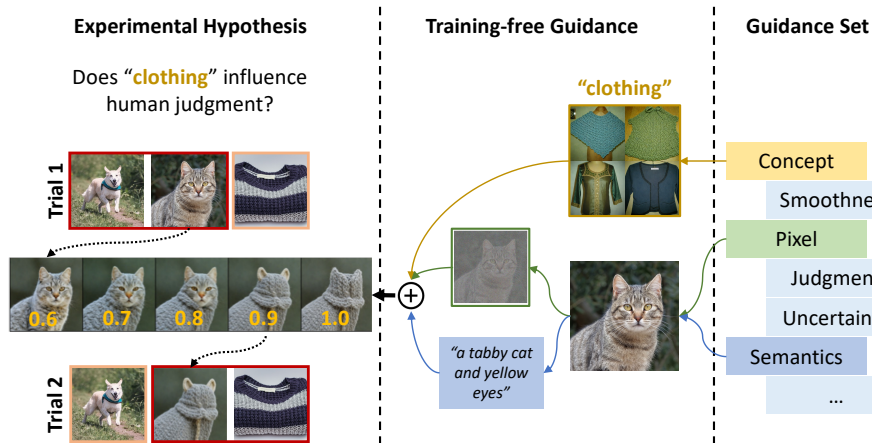


Fig. 1. Guided by the CoCoG-2, we can validate a specific hypothesis by generating visual stimuli in the controllable concept space using our framework. For instance, researchers propose an experimental hypothesis (*Does "clothing" influence human judgment?*), and then construct a loss function using a guidance set (aimed at preserving pixel and semantic features while modifying the concept of "clothing"), and finally generate alternative visual stimuli through training-free guidance (visual stimuli where the concept of "clothing" exceeds 0.9 lead to changes in human judgment). These synthetic images can be used to test the hypothesis with behavioral experiments .

key dimensions of concept representation. Previous studies have demonstrated that by controlling specific experimental inputs, we can directly observe the core factors that influence decision-making, a process referred to as counterfactual reasoning [18,4]. Similarly, by manipulating the concept representation within experimental stimuli, we can better uncover and understand the causal relationship between concept representations and behaviors. However, The concepts of complex natural visual stimuli often remain obscured and are quite challenging to manipulate. How to reveal the underlying concept space and generate the image by manipulating specific concepts remains largely unexplored.

Progress in controllable generation models has significantly shaped the AI field, especially through conditional generation models utilizing GANs and diffusion techniques [5,29,27,8,9]. Applications of these models span various domains such as text-to-image/video synthesis, image restoration, and biomedical imaging [22,20,11,2,14,26,17]. The generation conditions derive from diverse sources including text, sketches, and maps of edges, segmentation, or depth [22,20,14,35,34,1]. Despite these advances, the current models lack integration of human subjective inputs such as feelings or feedback, often resulting in outputs that do not align with human preferences. To better meet human expectations, recent studies have incorporated human feedback into these models, including visual preference scores and decisions from human-in-the-loop comparisons [31,12,23,3,28]. Furthermore, it is important to integrate human cognitive

mechanisms, such as decision-making based on concepts, into generative models. This integration can make the models more human-like and uncover human concept representations by manipulating concepts in generated images.

To generate images by controlling the concept space, a pioneer study, Wei et al. [30], has proposed a concept-based controllable generation (CoCoG) framework. CoCoG utilizes concept embeddings as conditions for the image generation model, thereby indirectly manipulating behaviors through concept representations. CoCoG comprises two parts: a concept encoder that learns concept embeddings by predicting human behaviors, and a concept decoder that maps concept embeddings to visual stimuli using a conditional diffusion model with a two-stage generation strategy. The concept encoder in CoCoG can accurately predict human visual similarity decision-making behaviors, revealing a reliable and interpretable space of human concept representations. The concept decoder can generate visual stimuli controlled by concept embeddings. The generated visual stimuli are highly consistent with the target concept embeddings and can regulate human similarity decision-making behaviors by manipulating concept dimensions. Notably, CoCoG preliminarily proposes efficiently exploring concept representations through generated visual stimuli, thus providing counterfactual explanations for human behavior. However, CoCoG has its limitations. CoCoG can only input complete concept embeddings as guiding conditions, leading to a lack of flexibility in guided generation. Firstly, CoCoG cannot edit the concepts of an image while keeping other image features unchanged, and conflicts may arise between concepts. Secondly, CoCoG cannot directly generate images based on expected similarity judgments and requires manually selecting "key concept" to guide image generation. These limitations restrict the method's further application in cognitive research based on concept representations.

In this study, we upgrade the CoCoG framework to CoCoG-2. CoCoG-2 allows us to design experimental stimuli based on concepts and effectively validate hypotheses about concept representation. Moreover, we employ a training-free guidance algorithm for the controllable generation of diffusion models with high flexibility. Our work has three main contributions.

- We present a general framework for designing experimental stimuli based on human concept representations and integrating experimental conditions through training-free guidance.
- We have verified a variety of potential guidance strategies for guiding the generation of visual stimuli, controlling concepts, behaviors, and other image features.
- Our experimental results demonstrate that visual stimuli generated by combining different guidance strategies can validate a variety of experimental hypotheses and enrich our tools for exploring concept representation.

2 Preliminaries

2.1 Training-free Guidance Diffusion Models

Diffusion Models. Diffusion models [27,10] operate through two distinct phases: the forward and the reverse processes. During the forward phase, which spans from time 0 to T , the model progressively converts an image into Gaussian noise. Conversely, during the reverse phase, it reconstructs the image starting from noise, reversing the timeline from T back to 0. Denote x_t as the state of the data at time t . In the forward phase, noise is methodically added according to a specific noise schedule:

$$x_t = a_t x_0 + b_t \epsilon_t, \quad (1)$$

where, $a_t = \sqrt{\alpha_t}$, $b_t = \sqrt{1 - \alpha_t}$, α_t varies monotonically from 0 to 1 as t increases, and ϵ_t is sampled from a standard normal distribution $\mathcal{N}(0, I)$. The neural network in diffusion models is trained to approximate the noise at each timestep:

$$\min_{\theta} \mathbb{E}_{x_t, \epsilon_t} [\|\epsilon_{\theta}(x_t, t) - \epsilon_t\|_2^2] = \min_{\theta} \mathbb{E}_{x_t, \epsilon_t} [\|\epsilon_{\theta}(x_t, t) + b_t \nabla_x \log p_t(x_t)\|_2^2], \quad (2)$$

where $p_t(x_t)$ represents the probability distribution of x_t . The dynamics of the reverse phase are governed by the following ordinary differential equation (ODE):

$$\frac{dx_t}{dt} = f(t)x_t - \frac{g^2(t)}{2} \nabla_x \log p_t(x_t) \quad (3)$$

with $f(t) = -\frac{d \log a_t}{dt}$ and $g^2(t) = \frac{db_t^2}{dt} - 2 \frac{d \log \sqrt{\alpha_t}}{dt} b_t^2$. Through these equations, the reverse process manages to transform Gaussian noise back into coherent images.

In practical applications, the update rules for both the forward and reverse processes depend on the choice of the sampling algorithm. In this work, we employ the DDPM algorithm [8] and we represent the forward and reverse steps using the following notations respectively:

$$x_t = DDPM^+(x_{t-1}) \quad \text{and} \quad x_{t-1} = DDPM^-(x_t).$$

Training-Free Guidance. In diffusion models, conditional generation introduces a specific condition y into the generative process [27,9]. By applying Bayes' rule $p(x|y) = \frac{p(y|x)p(x)}{p(y)}$, it incorporates the condition through an additional likelihood term $p(x_t|y)$:

$$\nabla_{x_t} \log p_t(x_t|y) = \nabla_{x_t} \log p_t(x_t) + \nabla_{x_t} \log p_t(y|x_t). \quad (4)$$

Recent approaches, known as training-free methods [2,1,34,25,32], utilize pre-trained diffusion models for conditional generation without the need for retraining or finetuning. These methods employ a pre-trained diffusion model and a differentiable loss function $\ell(f_\phi(x_0), y)$, defined using a neural network f_ϕ . Tweedie’s formula is used to compute $\nabla_{x_t} \log p_t(y|x_t)$ by estimating \hat{x}_0 from x_t :

$$\hat{x}_0(x_t) \approx \mathbb{E}[x_0|x_t] = \frac{x_t - b_t \epsilon_t(x_t, t)}{a_t}. \quad (5)$$

$$\nabla_{x_t} \log p_t(y|x_t) = \nabla_{x_t} \ell(f_\phi(\hat{x}_0(x_t)), y), \quad (6)$$

Then, we can add an additional correction step in the reverse sampling process:

$$x_{t-1} = DDPM^-(x_t) - \eta \nabla_{x_t} \ell(f_\phi(\hat{x}_0(x_t)), y)$$

This approximation allows the use of an existing network, which is initially trained for processing clean data (x_0). The gradient of the final term in the loss function is determined through backpropagation across the guidance network and the diffusion framework. In our example, where the condition is concept dimension, f_ϕ is modeled using a concept encoder, and ℓ is the loss designed for the experiment.

2.2 Concept based Controllable Generation

The CoCoG framework, introduced by Wei et al. [30], utilizes concept embeddings as conditional inputs for image generation, bridging cognitive science with artificial intelligence. CoCoG aims to enhance the production of natural visual stimuli in a controllable manner, closely aligning with human cognitive processes. It comprises two key components: a concept encoder for learning concept embeddings through human behavior prediction, and a concept decoder for transforming these embeddings into visual stimuli via a conditional diffusion model.

Concept Encoder The concept encoder extracts concept embeddings from visual objects. Each image x from a dataset is processed by the CLIP image encoder f to produce a CLIP embedding h . This embedding is then transformed by a learnable projector g into a concept embedding c :

$$\begin{aligned} \text{CLIP embedding:} \quad h &= f(x), \\ \text{concept embedding:} \quad c &= g(h), \end{aligned} \quad (7)$$

Each dimension of c corresponds to an interpretable concept, with its activation value reflecting the concept’s prominence in the visual object. Training is conducted using the *triplet odd-one-out* task from the THINGS dataset [6], employing dot product similarity and cross-entropy for decision prediction:

$$p(y) = \text{Softmax}(S_{jk}, S_{ik}, S_{ij}), \quad (8)$$

Here $S_{ij} = \langle c_i, c_j \rangle$, and predicted behavior y are matched against human judgments to train the projector g , with L_1 regularization ensuring sparsity in the concept embedding c .

Concept Decoder Following encoder training, triplets (x_i, h_i, c_i) are used by the concept decoder to control the generation of visual objects based on human concept representation. The process is formalized as:

$$p(x, h, c, y) = p(y)p(c|y)p(h|c)p(x|h). \quad (9)$$

The decoder operates in two phases. In stage I (prior diffusion), conditioned on c , a diffusion model learns the distribution of CLIP embeddings $p(h|c)$ using a lightweight U-Net $\epsilon_{prior}(h_t, t, c)$. The model trains on ImageNet pairs (h_i, c_i) using classifier-free guidance. In Stage II (CLIP-guided generation), with the CLIP embedding h from Stage I, a generator models $p(x|h)$ using pre-trained SDXL and IP-Adapter models [19,24,33], which facilitate the integration of h , to guide the U-Net’s denoising process.

CLIP Embedding as an Intermediate Variable They use CLIP embeddings as an intermediate variable for two reasons: 1) CLIP embeddings are low-level and retain key image information, effectively predicting human similarity judgments with linear probing [16]. 2) They enable the use of pre-trained generative models, adopting a two-stage generation strategy that requires only training a Prior Diffusion model, significantly reducing computational costs.

Despite its efficacy in generating controllable visual stimuli, CoCoG’s reliance on full concept embeddings for input restricts flexibility. It cannot modify specific concepts without altering other image attributes, leading to potential conflicts. Furthermore, it cannot generate images directly from predicted similarity judgments (i.e., $p(x|y)$), requiring manual selection of key concepts for image generation (i.e., $p(x|c = c(y))$), which limits its utility in detailed cognitive research. To address these limitations, further work should explore methods that allow for more flexible manipulation of specific concepts while maintaining control over other image attributes. For instance, generating multiple trials with consistent visual stimuli or varying only specific concepts without altering other features could be beneficial for more complex experimental designs. This improvement, which will be discussed below, would enhance CoCoG’s applicability in diverse research contexts.

3 Method

Compared to CoCoG, CoCoG-2 introduces improvements in the controllable generation strategy of the concept decoder. We simplify the distribution model from Equation 9 to $p(x, h, e) = p(e)p(h|e)p(x|h)$. Here, e represents the conditions that the visual stimuli need to be controlled, including concepts c , similarity judgments y , and others.

3.1 Training-free guidance for controlling visual stimuli

In the concept decoder of CoCoG-2, we continue to employ a two-stage strategy, first modeling $p(h|e)$ and then $p(x|h)$. In this work, we attempt to enhance the flexibility and applicability of CoCoG by introducing training-free guidance in the modeling of $p(h|e)$. As discussed in the Section 2.2, learning distribution $p(h|c)$ directly lacks flexibility. For training-free guidance, we only learn the prior distribution $p(h)$ and decompose $p(h|e)$ into the prior $p(h)$ and the likelihood $p(e|h)$ using Equation 4. As shown in Equation 6, for the likelihood term $p(e|h)$, we have $\nabla_{h_t} \log p_t(e|h_t) = \nabla_{h_t} \ell(f_\phi(\hat{h}_0(h_t)), e)$. By simply choosing the appropriate condition e and a differentiable loss function $\ell(f_\phi(\cdot), \cdot)$ based on the experimental hypothesis, we can effectively guide the generation of visual stimuli as demonstrated in Figure 1.

3.2 Guidance set and corresponding loss functions

To construct the loss function, we often wish for the visual stimuli to satisfy multiple conditions via guiding the generative process. We can combine our various requirements to construct an overall loss function $\ell = \sum \lambda_k \ell_k$, where λ_k controls the weight of each type of loss. Specifically, in our experiments, we will define the guidance set and their corresponding loss functions as follows:

Concept guidance: If we aim for the generated images to achieve predetermined concept values, we can define the loss function as:

$$\ell = \sum \|g(h)_i - c_i\| \quad (10)$$

where i indexes the concepts we wish to control, and c_i are their target values. We can control individual concepts or all concepts simultaneously (Like CoCoG).

Smoothness guidance: If we desire a batch of images to maintain semantic smoothness, we can define the loss function as:

$$\ell = \sum_{i,j \in S} \|h_i - h_j\| \quad (11)$$

Here, $S = \{i, j\}$ includes the indices of images in the batch that we want to remain smooth. For example, we can generate a batch of pairwise similar images (as shown in Figure 4).

Semantics guidance: To make the generated images similar to a given image semantically, we can define the loss function as:

$$\ell = \|h - \bar{h}\| \quad (12)$$

where \bar{h} is the CLIP embedding of the given image.

Judgment guidance: If we want human similarity judgments to follow a target judgment distribution, we can define the loss function as:

$$\ell = - \sum p(y = i) \log(\bar{p}(y = i)) \quad (13)$$

where $\bar{p}(y)$ is the target distribution. This loss function calculates the cross-entropy loss between the expected and target distributions. Given by Equation 8, $E_{p(y)}[y] = \text{Softmax} \cdot S \cdot g(h)$, so ℓ is still a derivable function with respect to h .

Uncertainty guidance: When we need to control the uncertainty in similarity judgments, we can define the loss function using the entropy of the expected judgment distribution:

$$\ell = H(p(y)) = - \sum p(y = i) \log(p(y = i)) \quad (14)$$

Pixel guidance: Since CLIP embedding h primarily controls the high-level features or semantic features of the generated images, we also try to introduce `img2img` [14] to control the low-level features of the images.

3.3 Improving Training-Free Guidance

Previous research has indicated that the generation process of training-free guidance is unstable and prone to guidance failures. To ensure the stability and effectiveness of guidance, we analyzed recent major advancements in this area and employed two techniques to enhance training-free guidance.

Adaptive gradient scheduling. Inspired by [25,32], the training guidance process can be viewed as optimizing the loss function of the guidance network. It stands to reason that adopting a more sophisticated optimizer could accelerate the convergence of the guidance. Following [32], we use a closed-form solution based on the spherical Gaussian constraint:

$$h_{t-1}^* = h_t - \eta \sqrt{n} \sigma_t \frac{\nabla_{h_t} \ell(f_\phi(\hat{h}_0(h_t)), e)}{\|\nabla_{h_t} \ell(f_\phi(\hat{h}_0(h_t)), e)\|_2}, \quad (15)$$

where $\sigma_t = \sqrt{(1 - \alpha_{t-1}) / (1 - \alpha_t)} \sqrt{1 - \alpha_t / \alpha_{t-1}}$, n is the dimension of the h , and η is the guidance scale.

Resampling trick. Following [34,25], we use resampling, or “time travel”, to address sampling errors. This involves reintroducing random noise to reset the sampling state, reducing distributional divergence and aligning samples with the target distribution.

Algorithm 1 Improved training-free guidance for prior diffusion

```

1: for  $t = T, \dots, 0$  do
2:   for  $i = 1, \dots, s$  do
3:      $h_{t-1}^i = DDPM^-(h_t^i)$ 
4:      $\hat{h}_0^i = \frac{h_t^i - \sigma_t \epsilon_\theta(h_t^i, t)}{\sqrt{\alpha_t}}$ 
5:      $g_t = \nabla_{h_t} \ell(f_\phi(\hat{h}_0^i(h_t^i)), e)$ 
6:      $h_{t-1}^i = h_{t-1}^i - \eta \sqrt{n} \sigma_t \frac{g_t}{\|g_t\|_2}$ 
7:     if  $i < s$  then
8:        $h_t^i = DDPM^+(h_{t-1}^i)$ 
9:     end if
10:     $h_{t-1}^0 \leftarrow h_{t-1}^s$ 
11:  end for
12: end for

```



Fig. 2. Generate diverse visual stimuli for given target concepts. (a) Concept guidance used in this experiment. (b) Visual stimuli generated under the guidance of one or more target concepts.

4 CoCoG-2 for versatile experiment design

4.1 Diverse generation based on concept

In the first experiment, we tested the effectiveness of using CoCoG-2 to generate visual stimuli based on given target concepts. The objective of the experiment was to generate diverse samples specific activation values of single or multiple concept dimensions. Therefore we only used *Concept guidance* to guide the Prior Diffusion. As shown in Figure 2b, whether guided by a single concept or multiple concepts, CoCoG-2 was able to generate images that were well-aligned with the target concepts, and these images exhibited good diversity in features unrelated to given concept.

4.2 Smooth changes based on concepts

After confirming that target concepts can effectively guide the generation of visual stimuli, we modified the activation values of target concepts in the second experiment to generate a group of stimuli while maintaining smooth semantic features. We used *Concept guidance* to allow gradual changes in concept activation

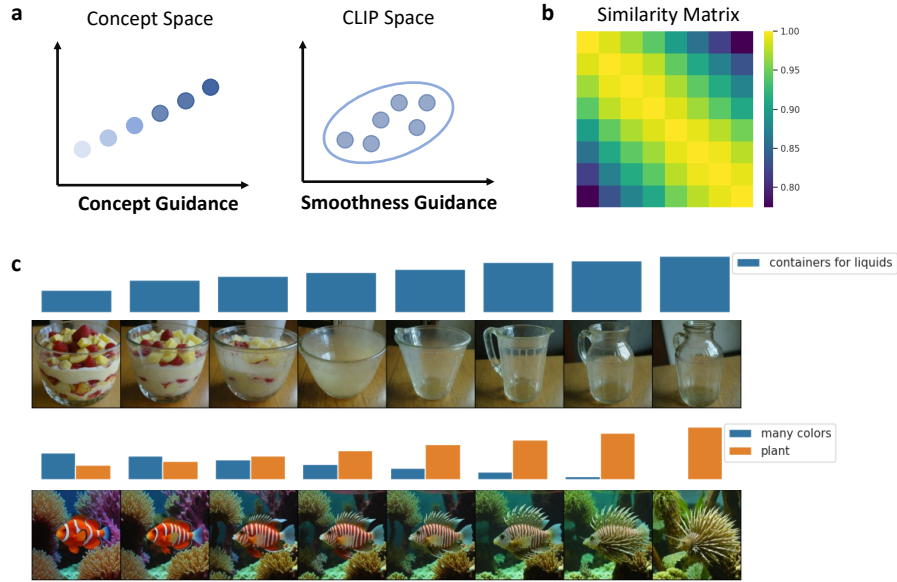


Fig. 3. The smooth change of visual stimuli generated based on concept. (a) Concept guidance and Smoothness guidance used in this experiment. (b) The average CLIP similarity matrix of 100 groups of stimuli. (c) Two trials of images generated under the guidance of one or more target Concepts.

values and employed *Smoothness guidance* to maintain the similarity of semantic features between neighboring stimuli. We randomly generated 50 groups of visual stimuli and calculated the similarity matrix of CLIP embeddings for each group’s stimuli, which was then averaged to obtain a mean similarity matrix. The similarity matrix shown in Figure 3b indicates that the CLIP similarity of images within a trial ranged between 0.75 and 1.0, with similarity increasing as the distance of image position decreased, consistent with the expected effect of Smoothness guidance. Figure 3c displays visual stimuli generated under the guidance of one or more varying target concepts, showing clear and stable changes at the concept level, while other features were well maintained.

4.3 Image editing in concept

Next, we tested whether it was possible to start with an "original image" and edit target concepts to generate a group of stimuli that are similar to the original image and vary the concepts according to given values. For concept editing, we used *Concept guidance*; to maintain other features of images within a trial, we applied *Smoothness guidance*. Additionally, we utilized *Semantics guidance* in CLIP Space and *Pixel guidance* in Pixel Space to maximize the similarity between the generated images and the original image.

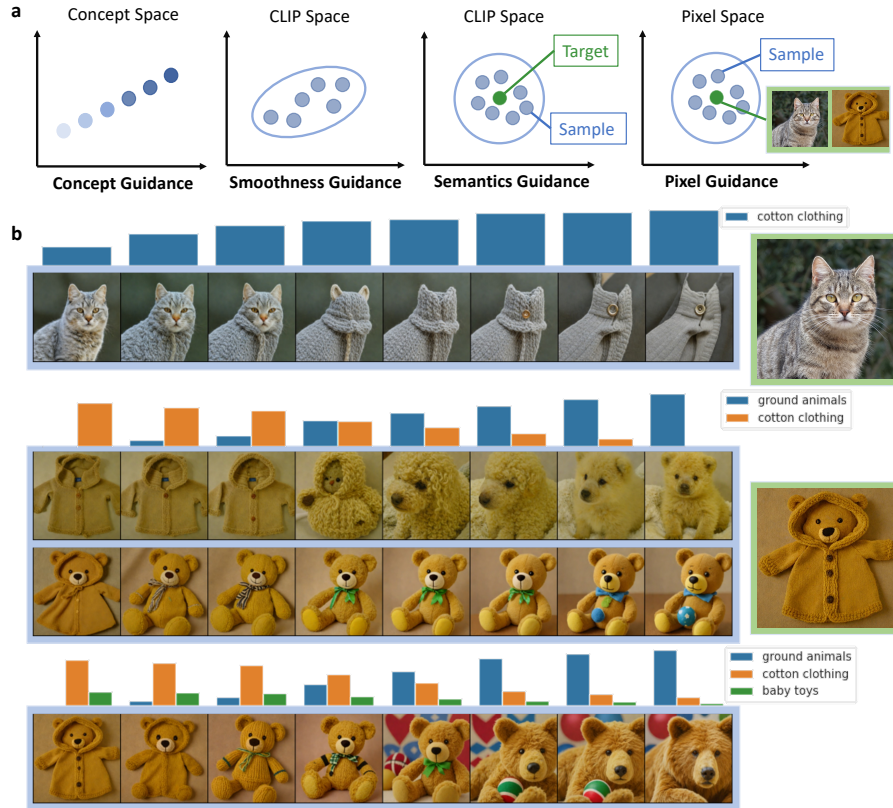


Fig. 4. Visual stimuli generated by image editing in concept. (a) *Concept*, *Smoothness*, *Semantics*, and *Pixel guidance* used in this experiment. (b) A trial of images generated under the guidance of a single concept (row 1); Visual stimuli generated by CoCoG-2 and CoCoG under the guidance of multiple concepts (row 2-4). When guided only by "ground animals" and "cotton clothing," the images generated by CoCoG-2 align well with the target concepts. However, the images generated by CoCoG cannot produce real animals due to conflicts between target concepts and the concept "baby toys" in the original image, necessitating manual adjustment of the "baby toys" value.

As shown in Figure 4b, Visual stimuli generated by CoCoG-2 not only resembled the original image but also achieved clear and stable concept edits, with well-preserved low-level features. This experiment also highlighted a significant advantage of CoCoG-2 over CoCoG: it can automatically avoid conflicts between target concepts and the concepts in the original image, without the need for manually modifying conflicting concepts. As shown in rows 2-3 of Figure 4b, both guided by "ground animals" and "cotton clothing", CoCoG-2 was able to generate real animals, whereas CoCoG could only generate fabric toy bears. This is because the concept "baby toys" in the original image conflicted with target

concepts. Even if the activation value of "cotton clothing" was set to zero, the generated images still contained this concept. Therefore, as shown in row 4 of Figure 4b, it was necessary to manually modify the activation value of "baby toys" to generate real animals.

CoCoG's manual modification process increased the complexity of visual stimuli generation, as conflicting concepts had to be identified and modified through multiple rounds of generation, and it is possible that contradictions could not be resolved by altering just a few key concepts. However, CoCoG-2's Training-Free Guidance method could automatically adjust conflicting concepts, greatly speeding up the generation process.

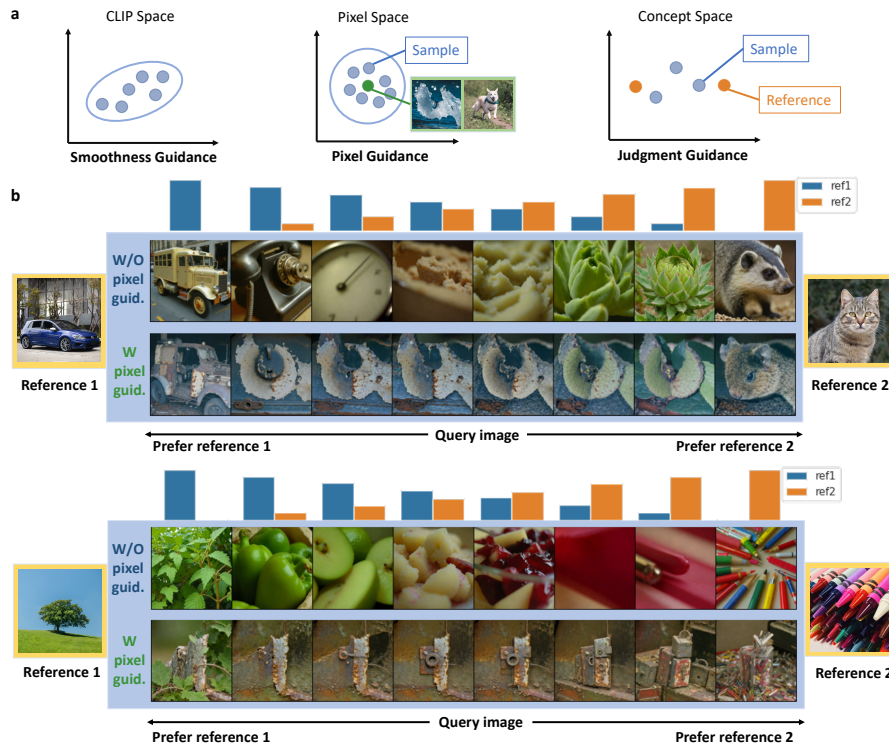


Fig. 5. Behavioral manipulation of similarity judgments with/without *Pixel guidance*. (a) *Smoothness*, *Pixel*, and *Judgment guidance* used in this experiment. (b) Images generated under the guidance of probability interpolation of two pairs of references. The top row of images for each set is generated without using the *Pixel guidance*, while the bottom row of images is generated with the *Pixel guidance*.

4.4 Behavioral manipulation of similarity judgment

After verifying CoCoG-2’s capability of concept editing based on the original image, we further tested whether CoCoG-2 could directly generate visual stimuli guided by experimental results. We used the *Two alternative forced choice* experiment as an example, where participants need to choose between reference 1 & 2, judging which is more similar to a query. In this scenario, the experimental results can be represented as the probability of choosing reference 1 or 2 as the more similar image. We used the probabilities of each reference image being chosen as the guidance, termed the *Judgment guidance*. Additionally, to study the causal relationship between visual cognitive behavior and concept representation, we needed to ensure that changes of behavioral results were solely caused by changes in concepts, which means maintaining other features of the images. Therefore, we used the *Smoothness guidance* to maintain other features within a group, and guided the query image’s low-level features using an image unrelated to the reference images, termed the *Pixel guidance*.

In Figure 5b, we show the generated query images for two references. The upper group of each set is without the *Pixel guidance*, and significant variations in low-level features can be observed among the generated images. The lower group is with the *Pixel guidance*, where the images in Figure 5a labeled "ice" and "dog" were used to guide the low-level features respectively. Both groups of image align with the given results of similarity judgment. However, the lower group of images also maintains consistency with the guiding images in shape, color, and other low-level features. This greatly reduces the impact of low-level features on behavioral results, more reliably interpreting the causal relationship between behavior and concepts.

4.5 Optimal design for individual preference

We demonstrated that CoCoG-2 can directly generate images guided by behavioral results, significantly facilitating the rapid production of desirable experimental outcomes. Beyond this, CoCoG-2 can also be used to design and generate visual stimuli that maximize information gain, thereby substantially reducing the number of experimental trials required in cognitive research. Taking individual preferences in the *Two alternative forced choice* experiment as an example, for the same set of inference images and query image, each participant may choose a different inference image as the more similar one. The greater the variance in participants’ choices, and the more information each experiment can provide about individual preferences. Therefore, when the entropy of the probability distribution for choosing between the two reference images is maximized, each *Two alternative forced choice* experiment provides the maximum information gain.

Furthermore, we consider each experiment’s three images from the perspective of the *Odd One Out* experiment. The *Odd One Out* experiment is a triplet choice task where participants select the image that is least similar to the others as the odd one out. This experiment can reveal the similarity relationships between the three images, and its results can be represented by the probability of

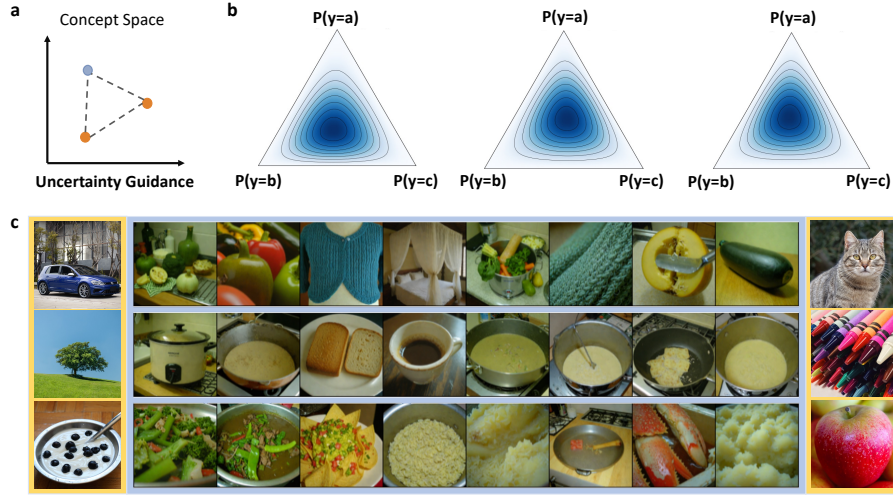


Fig. 6. Generated trials of similarity judgment leading to rich individual preference information. (a) *Uncertainty guidance* used in this experiment. (b) Probability distributions of three sets of generated images in c, with each side of the triangle representing the probability of choosing a particular image as the odd one out. (c) Images generated under the guidance of *Uncertainty guidance* for three pairs of references.

each image being selected as the odd one out. Therefore, when the entropy of the probability distribution for the three images being chosen as the odd one out is maximized, each Odd One Out experiment provides the maximum information gain.

Consequently, our optimization goal is to maximize the entropy of the probability distribution for the three images being chosen as the odd one out, guided by *Uncertainty guidance*. The choice probability is determined by the similarity between the images, which in turn is dictated by their relative distances in Concept Space. Maximizing the entropy of the probability distribution implies that the three images form an equilateral triangle in Concept Space, as shown in Figure 6a. Since Concept Space has 42 dimensions, there can be at most 43 possible query images that meet the equilateral triangle condition. Figure 6c displays generated images corresponding to three pairs of reference images. These generated images are positioned at the vertices of multiple equilateral triangles in the 42-dimensional space, exhibiting good diversity. Additionally, Figure 6b shows the probability distribution for these three sets of images, with the distribution centers very close to the center of the equilateral triangle, indicating that the generated images well satisfy the target probability distribution. These images are diverse and informative, making them optimal experimental images for studying individual preferences.

5 Discussion

In conclusion, our proposed CoCoG-2 framework advances the field of controllable visual object generation by integrating concept representations with behavioral outcomes to guide the image generation process. By employing a versatile experiment designer and utilizing meticulously designed guidance, CoCoG-2 not only addresses the limitations of its predecessor, CoCoG, but also significantly enhances the flexibility and efficiency of generating visual stimuli for cognitive research. The experimental trials generated using CoCoG-2 are instrumental in probing the causal relationships between concept representations and human decision-making behaviors. This approach marks a substantial step towards understanding and manipulating concept-based representations in a controllable and meaningful way, offering a robust methodology for cognitive science research and practical applications in AI-driven visual content generation.

Ethical Statement

The human behavioral data in this study is from THINGS public dataset. No animal or human experiments are involved.

References

1. Bansal, A., Chu, H.M., Schwarzschild, A., Sengupta, S., Goldblum, M., Geiping, J., Goldstein, T.: Universal guidance for diffusion models. In: Proceedings of the IEEE/CVF Conference on Computer Vision and Pattern Recognition. pp. 843–852 (2023)
2. Chung, H., Sim, B., Ryu, D., Ye, J.C.: Improving diffusion models for inverse problems using manifold constraints. *Advances in Neural Information Processing Systems* **35**, 25683–25696 (2022)
3. Fan, Y., Watkins, O., Du, Y., Liu, H., Ryu, M., Boutilier, C., Abbeel, P., Ghavamzadeh, M., Lee, K., Lee, K.: Dpok: Reinforcement learning for fine-tuning text-to-image diffusion models. *arXiv preprint arXiv:2305.16381* (2023)
4. Fernández-Loría, C., Provost, F., Han, X.: Explaining data-driven decisions made by ai systems: the counterfactual approach. *arXiv preprint arXiv:2001.07417* (2020)
5. Goodfellow, I., Pouget-Abadie, J., Mirza, M., Xu, B., Warde-Farley, D., Ozair, S., Courville, A., Bengio, Y.: Generative adversarial networks. *Communications of the ACM* **63**(11), 139–144 (2020)
6. Hebart, M.N., Contier, O., Teichmann, L., Rockter, A.H., Zheng, C.Y., Kidder, A., Corriveau, A., Vaziri-Pashkam, M., Baker, C.I.: Things-data, a multimodal collection of large-scale datasets for investigating object representations in human brain and behavior. *Elife* **12**, e82580 (2023)
7. Hebart, M.N., Zheng, C.Y., Pereira, F., Baker, C.I.: Revealing the multidimensional mental representations of natural objects underlying human similarity judgements. *Nature human behaviour* **4**(11), 1173–1185 (2020)
8. Ho, J., Jain, A., Abbeel, P.: Denoising diffusion probabilistic models. *Advances in neural information processing systems* **33**, 6840–6851 (2020)

9. Ho, J., Salimans, T.: Classifier-free diffusion guidance. arXiv preprint arXiv:2207.12598 (2022)
10. Karras, T., Aittala, M., Aila, T., Laine, S.: Elucidating the design space of diffusion-based generative models. *Advances in Neural Information Processing Systems* **35**, 26565–26577 (2022)
11. Kawar, B., Elad, M., Ermon, S., Song, J.: Denoising diffusion restoration models. *Advances in Neural Information Processing Systems* **35**, 23593–23606 (2022)
12. Kirstain, Y., Polyak, A., Singer, U., Matiana, S., Penna, J., Levy, O.: Pick-a-pic: An open dataset of user preferences for text-to-image generation. arXiv preprint arXiv:2305.01569 (2023)
13. Medin, D.L., Goldstone, R.L., Gentner, D.: Respects for similarity. *Psychological review* **100**(2), 254 (1993)
14. Meng, C., He, Y., Song, Y., Song, J., Wu, J., Zhu, J.Y., Ermon, S.: Sdedit: Guided image synthesis and editing with stochastic differential equations. In: *International Conference on Learning Representations* (2021)
15. Murphy, G.L., Medin, D.L.: The role of theories in conceptual coherence. *Psychological review* **92**(3), 289 (1985)
16. Muttenthaler, L., Dippel, J., Linhardt, L., Vandermeulen, R.A., Kornblith, S.: Human alignment of neural network representations. In: *The Eleventh International Conference on Learning Representations* (2022)
17. Özbey, M., Dalmaz, O., Dar, S.U., Bedel, H.A., Öztürk, Ş., Güngör, A., Çukur, T.: Unsupervised medical image translation with adversarial diffusion models. *IEEE Transactions on Medical Imaging* (2023)
18. Peterson, J.C., Bourgin, D.D., Agrawal, M., Reichman, D., Griffiths, T.L.: Using large-scale experiments and machine learning to discover theories of human decision-making. *Science* **372**(6547), 1209–1214 (2021)
19. Podell, D., English, Z., Lacey, K., Blattmann, A., Dockhorn, T., Müller, J., Penna, J., Rombach, R.: Sdxl: Improving latent diffusion models for high-resolution image synthesis. arXiv preprint arXiv:2307.01952 (2023)
20. Ramesh, A., Dhariwal, P., Nichol, A., Chu, C., Chen, M.: Hierarchical text-conditional image generation with clip latents. arXiv preprint arXiv:2204.06125 **1**(2), 3 (2022)
21. Roads, B.D., Love, B.C.: Modeling similarity and psychological space. *Annual Review of Psychology* **75** (2023)
22. Rombach, R., Blattmann, A., Lorenz, D., Esser, P., Ommer, B.: High-resolution image synthesis with latent diffusion models. In: *Proceedings of the IEEE/CVF conference on computer vision and pattern recognition*. pp. 10684–10695 (2022)
23. von Rütte, D., Fedele, E., Thomm, J., Wolf, L.: Fabric: Personalizing diffusion models with iterative feedback. arXiv preprint arXiv:2307.10159 (2023)
24. Sauer, A., Lorenz, D., Blattmann, A., Rombach, R.: Adversarial diffusion distillation. arXiv preprint arXiv:2311.17042 (2023)
25. Shen, Y., Jiang, X., Wang, Y., Yang, Y., Han, D., Li, D.: Understanding training-free diffusion guidance: Mechanisms and limitations. arXiv preprint arXiv:2403.12404 (2024)
26. Song, Y., Shen, L., Xing, L., Ermon, S.: Solving inverse problems in medical imaging with score-based generative models. In: *International Conference on Learning Representations* (2021)
27. Song, Y., Sohl-Dickstein, J., Kingma, D.P., Kumar, A., Ermon, S., Poole, B.: Score-based generative modeling through stochastic differential equations. In: *International Conference on Learning Representations* (2020)

28. Tang, Z., Rybin, D., Chang, T.H.: Zeroth-order optimization meets human feedback: Provable learning via ranking oracles. arXiv preprint arXiv:2303.03751 (2023)
29. Tao, M., Tang, H., Wu, F., Jing, X.Y., Bao, B.K., Xu, C.: Df-gan: A simple and effective baseline for text-to-image synthesis. In: Proceedings of the IEEE/CVF Conference on Computer Vision and Pattern Recognition. pp. 16515–16525 (2022)
30. Wei, C., Zou, J., Heinke, D., Liu, Q.: Cocog: Controllable visual stimuli generation based on human concept representations. arXiv preprint arXiv:2404.16482 (2024)
31. Wu, X., Sun, K., Zhu, F., Zhao, R., Li, H.: Human preference score: Better aligning text-to-image models with human preference. In: Proceedings of the IEEE/CVF International Conference on Computer Vision. pp. 2096–2105 (2023)
32. Yang, L., Ding, S., Cai, Y., Yu, J., Wang, J., Shi, Y.: Guidance with spherical gaussian constraint for conditional diffusion. arXiv preprint arXiv:2402.03201 (2024)
33. Ye, H., Zhang, J., Liu, S., Han, X., Yang, W.: Ip-adapter: Text compatible image prompt adapter for text-to-image diffusion models. arXiv preprint arXiv:2308.06721 (2023)
34. Yu, J., Wang, Y., Zhao, C., Ghanem, B., Zhang, J.: Freedom: Training-free energy-guided conditional diffusion model. arXiv preprint arXiv:2303.09833 (2023)
35. Zhang, L., Rao, A., Agrawala, M.: Adding conditional control to text-to-image diffusion models. In: Proceedings of the IEEE/CVF International Conference on Computer Vision. pp. 3836–3847 (2023)